NASA Technical Memorandum 110278
U. S. Army Research Laboratory Technical Report 1213

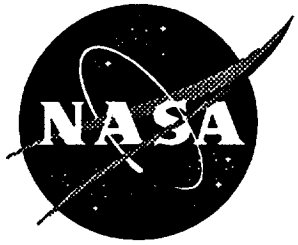

Analysis of Thick Sandwich Shells With Embedded Ceramic Tiles

Carlos G. Davila
Vehicle Structures Directorate
U.S. Army Research Laboratory
Langley Research Center, Hampton, Virginia

C. Smith and F. Lumban-Tobing
United Defense, San Jose, California

September 1996

National Aeronautics and
Space Administration
Langley Research Center
Hampton, Virginia 23681-0001

Analysis of Thick Sandwich Shells with Embedded Ceramic Tiles

C. G. Dávila
Vehicle Structures Directorate, U.S. Army Research Laboratory
NASA Langley Research Center, Hampton, VA

C. Smith and F. Lumban-Tobing
United Defense (FMC/BMY), San Jose, CA

Abstract

The Composite Armored Vehicle (CAV) is an advanced technology demonstrator of an all-composite ground combat vehicle. The CAV upper hull is made of a tough light-weight S2-glass/epoxy laminate with embedded ceramic tiles that serve as armor. The tiles are bonded to a rubber mat with a carefully selected, highly viscoelastic adhesive. The integration of armor and structure offers an efficient combination of ballistic protection and structural performance. The analysis of this anisotropic construction, with its inherent discontinuous and periodic nature, however, poses several challenges. The present paper describes a shell-based "element-layering" technique that properly accounts for these effects and for the concentrated transverse shear flexibility in the rubber mat. One of the most important advantages of the element-layering technique over advanced higher-order elements is that it is based on conventional elements. This advantage allows the models to be portable to other structural analysis codes, a prerequisite in a program that involves the computational facilities of several manufacturers and government laboratories. The element-layering technique was implemented into an auto-layering program that automatically transforms a conventional shell model into a multi-layered model. The effects of tile layer homogenization, tile placement patterns, and tile gap size on the analysis results are described.

Introduction

Virtually every aerospace company and many land-vehicle manufacturers are developing products made with fiber-reinforced composite materials. In the last thirty years, the use of composite materials has progressed through several stages. The early stages consisted of replacing a metallic component with a similarly designed composite part. The current stage of composite material usage is the all-composite vehicle. This long-held vision is now possible with the development of new fundamental insight into the mechanics issues of composite structures along with new analytical and computational tools. The Composite Armored Vehicle is an advanced technology demonstrator that is fabricated using tough light-weight S2-glass/epoxy laminates with embedded ceramic tiles. To the analyst, however, the juxtaposition of materials with very different stiffnesses poses computational

difficulties unlike those of typical composite structures. It was found that standard finite element techniques provide inaccurate results for this type of construction. The first section of the present paper describes the response characteristics of the CAV upper hull determined from the results of an analysis of a three-dimensional (3D) finite element model. Then, the limitations of conventional shell elements as applied to the CAV laminates are discussed. Finally, the element-layering technique and the homogenization of the tile-adhesive layer are demonstrated to be accurate and efficient for use in global analyses of tile-reinforced armored vehicles.

Response Characteristics of the CAV Upper Hull

The core of the CAV upper hull consists of 0.7-inch-thick, 4-inch-by-4-inch-square Al_2O_2 ceramic tiles. The CAV upper hull achieves its ballistic performance though the complex interaction of brittle ceramic tiles, tough S2-glass/epoxy plies, and low modulus rubber and adhesive materials. The differences in moduli and size occur in both the thickness and the in-plane directions, as can be observed in Fig. 1. The strain distributions in this structure are quite different from what might be expected in an isotropic structure. In particular, two aspects of tile-reinforced laminates pose challenges to the analysis. The first difficulty is due to the variation of properties in the thickness direction; the other is due to the variation of properties in-plane. The softness of the rubber mat allows some relative motion to occur between the upper and lower portions of the laminate. This relative motion invalidates the assumptions used for conventional shell finite elements. The problem was solved in the present paper with the method of "element-layering." Furthermore, adhesive gaps are too small to be modeled in a practical global model. Therefore, macroscopically equivalent material properties were determined for a tile layer in which the tiles and adhesive gaps are smeared.

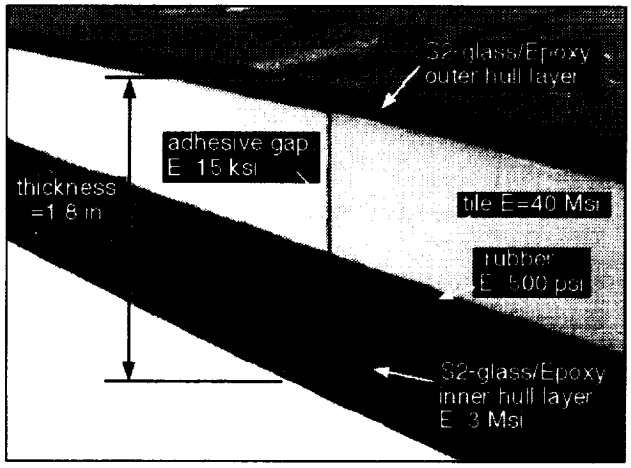

Figure 1. Photograph of the edge of a CAV upper hull specimen. Approximate values of Young's moduli illustrate the large variations in properties between adjacent materials.

Solid elements are essential to compute three-dimensional stress fields. A detail of a three-dimensional model of a CAV laminate beam subjected to three-point bending is shown in Fig. 2. The model is symmetric at mid-span. The symmetry plane and the applied loads on the upper edge of this plane are also shown in Fig. 2. The fringes on the model correspond to the axial stress contours, and it can be observed that the tiles have by far the highest stresses.

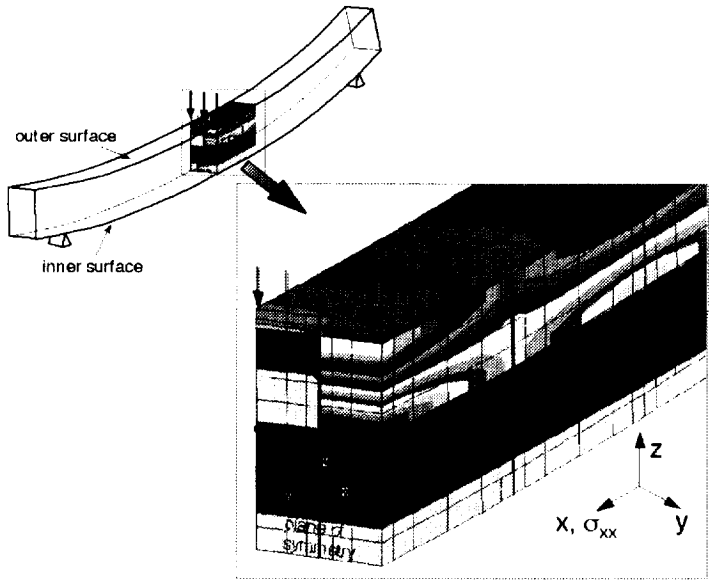

Figure 2. Detail of three-dimensional model of laminate beam subjected to three-point bending. Contours indicate stress concentrations in tiles.

The deformation of the beam subjected to three-point bending is shown in Fig. 3. It can be observed that the beam deforms less like a monolithic structure than like two loosely coupled laminates, one on top of the other.

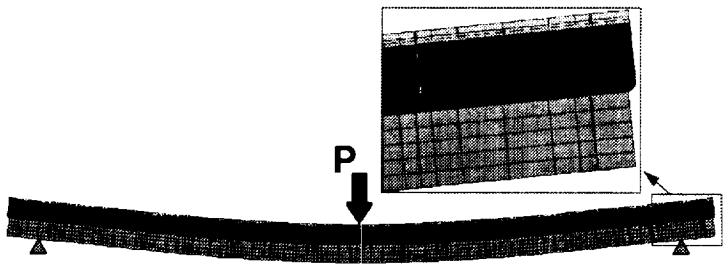

Figure 3. Three-dimensional model of a CAV beam subjected three-point bending. Free edges of beam display transverse shearing of rubber layer.

In addition to the changes in material properties through-the-thickness from a tile to the rubber mat, there is also an in-plane periodicity due to the adhesive-filled gaps between tiles. The tiles are aligned in a pattern consisting of staggered rows. The bondline is many times smaller than the length of a tile, yet its low

stiffness produces as much elongation as the tile, as can be seen from the deformations shown in Fig. 4.

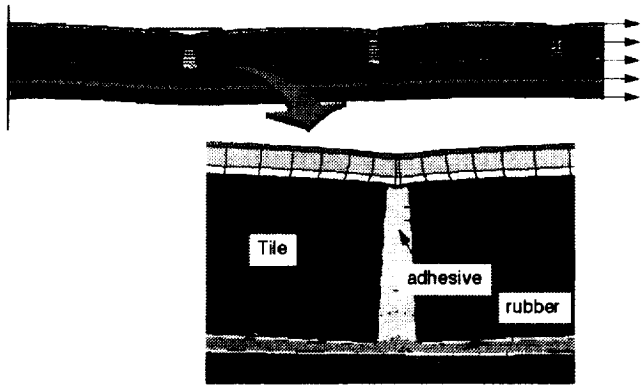

Figure 4. Plane strain analysis of sandwich beam in tension. High compliance of the small adhesive bondline results in a relatively large opening of the gap.

While three-dimensional models are often the only means of predicting complex stress fields, they are currently so computationally expensive that they are impractical for the analysis of anything other than small and relatively simple components.

Analysis of CAV Upper Hull Laminates with Shell Elements

Most finite element analyses of thick composite structures rely on so-called thick-shell elements. These computationally efficient elements are based on the Mindlin-Reissner (MR) kinematic assumptions that state that the normal to the shell remains straight and does not elongate. The MR assumptions imply that the transverse shear in the shell is constant through the thickness, and this theory is referred to as a First Order Transverse Shear Deformation Theory (FSDT). One inconsistency in this theory is that the constant transverse shear does not satisfy the traction-free boundary conditions at the top and bottom faces of the laminate. This inconsistency is offset by applying a shear correction factor (SCF) to the transverse shear stiffnesses. For isotropic materials, where the transverse shear distribution due to a static load is exactly parabolic, the SCF is 5/6. Whitney[1] and others have proposed methods to compute the SCF for non-isotropic materials, and it may seem reasonable to expect that it is possible to compute a SCF for the CAV laminate. The following discussion shows that it is not possible to compute a single SCF for all CAV analyses. The results of an analysis of a three-point-bending model for various SCFs are shown in Fig. 5. The stiffness of the plate is plotted as a function of the SCF. A SCF of 5/6 results in an overly stiff response that corresponds to the response of a monolithic plate. Whitney's method results in a SCF of only 0.04 and causes an overly compliant deformation that almost corresponds to a beam with pure shear deformation that has near-zero slope outboard of the supports and deflection without bending inboard of the supports. A comparison with experimental results suggests that a SCF of 0.1 is

appropriate, but it can be shown that this number is a function of specimen length. In other words, the unusual through-the-thickness strain distributions in laminates with embedded tiles cannot be represented by conventional shell elements, and conventional SCFs are incapable of accounting for the concentration of transverse shear in the rubber layer without unbalancing the ratio of shearing and bending energies.

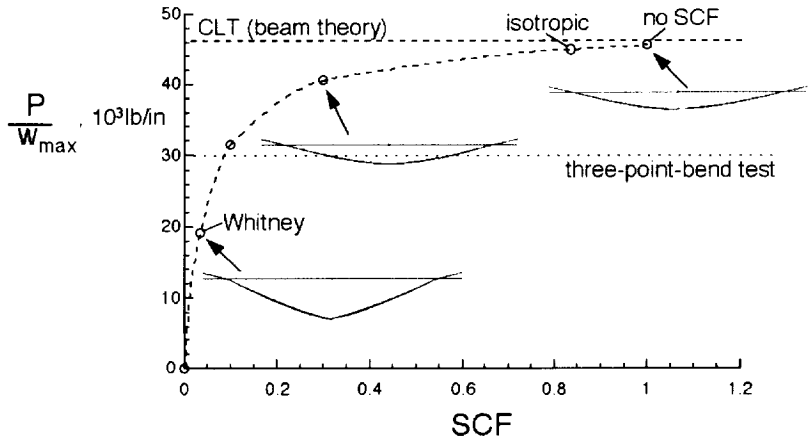

Figure 5. Effect of shear correction factor on the global stiffness and bending mode of a 33-inch-long by 16-inch-wide plate in three-point bending, with a 27-inch-long support span.

Element-Layering for Higher-Order Transverse Deformation

Shell elements of high order in transverse shear are becoming relatively common in research codes. Averill's shell elements[2] with high-order zig-zag sublaminate approximations, for instance, can even simulate delaminations by using plies of nearly zero material stiffness. However, higher-order elements usually possess a large number of degrees-of-freedom per node, which renders their implementation into commercial finite element codes rather complex. Furthermore, the present study involves the cooperative analysis efforts and computational facilities of several manufacturers and government laboratories, so a solution to the lack of accuracy of shell elements has to be compatible with typical commercial finite element codes. The solution adopted here consists of a new method of "element-layering," which is similar to a method used to compute fracture parameters and interlaminar stresses in skin-stiffener debond problems.[3-4] Element-layering is designed to provide the needed higher order in transverse displacements. The method simply consists of modeling the laminated composite shell with more than one thick-shell element through the thickness, each element layer comprising a sublaminate of similar components. For instance, the CAV upper hull laminate can be layered into four element layers: 1) a glass-epoxy inner-hull layer; 2) a rubber layer; 3) a tile layer; and 4) an outer glass-epoxy layer. The layers are tied together in the model with multi-point constraint equations (MPC) that enforce displacement compatibility at the layer interfaces. Continuity requires that the displacements on both sides of the common interface

between two regions be equal. MPC's do not model the stiffness of the adhesive gap, but rather the compatibility of displacements at the boundary surface separating two arbitrary regions. Using the Mindlin-Reissner kinematic equations of FSDT, the MPCs at an interface are

$$\begin{aligned} u_l + \tfrac{t_l}{2}\theta_l^y &= u_u - \tfrac{t_u}{2}\theta_u^y \\ v_l - \tfrac{t_l}{2}\theta_l^x &= v_u + \tfrac{t_u}{2}\theta_u^x \\ w_l &= w_u \end{aligned} \tag{1}$$

where u_u and u_l are the displacements of the layers above and below the interface, and θ_u and θ_l are the rotations of the layers above and below the interface, respectively, as shown in Fig. 6.

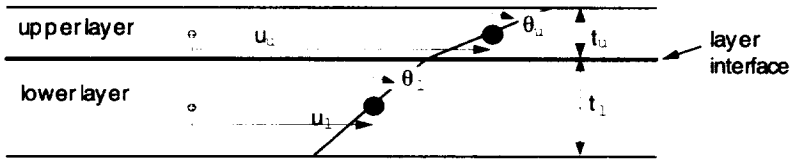

Figure 6. Multi-Point Constraints consistant with the Mindlin-Reissner kinematics of FSDT are used to enforce displacement continuity at the interface between two bonded layers. The displacements at the interface are functions of the translation component, u, the rotation, θ, and the thickness of the layer, t.

Most finite element codes require the separation of the degrees-of-freedom into dependent and independent degrees-of-freedom u_i and u_d, respectively. The separation is achieved by partitioning the constraint equation matrix as

$$\begin{bmatrix} M_i & M_d \end{bmatrix} \begin{Bmatrix} u_i \\ u_d \end{Bmatrix} = \begin{Bmatrix} 0 \\ 0 \end{Bmatrix} \quad \Rightarrow \quad u_d = -M_d^{-1} M_i u_i \tag{2}$$

For instance, after separation of the dependent and independent degrees-of-freedom, the x-direction MPC's for a four-layer model can be written as

$$\begin{Bmatrix} \frac{t_2}{2}\theta_2^y \\ \frac{t_3}{2}\theta_3^y \\ \frac{t_4}{2}\theta_4^y \end{Bmatrix}_{dependent} = \begin{bmatrix} -1 & 1 & 0 & 0 & -1 \\ 1 & -2 & 1 & 0 & 1 \\ -1 & 2 & -2 & 1 & -1 \end{bmatrix} \begin{Bmatrix} u_1 \\ u_2 \\ u_3 \\ u_4 \\ \frac{t_1}{2}\theta_1^y \end{Bmatrix}_{independent} \tag{3}$$

Element-layering introduces two additional degrees of freedom per node for each additional layer. If a conventional model has six degrees of freedom per node, a two-layer model has eight, and a four-layer model has twelve. Note that that element-layering does not require SCFs since the transverse shear distribution is nearly constant in each layer, especially in the thin rubber mat, which is near the center of the laminate.

A comparison between the results for a layered model and for a three-dimensional *(3D)* model in bending is shown in Fig. 7. The left portion of the figure shows three four-layer shell models of varying support spans, Ls. The right portion of the figure shows the corresponding *3D* model. The agreement between the two types of models is excellent for all three support spans.

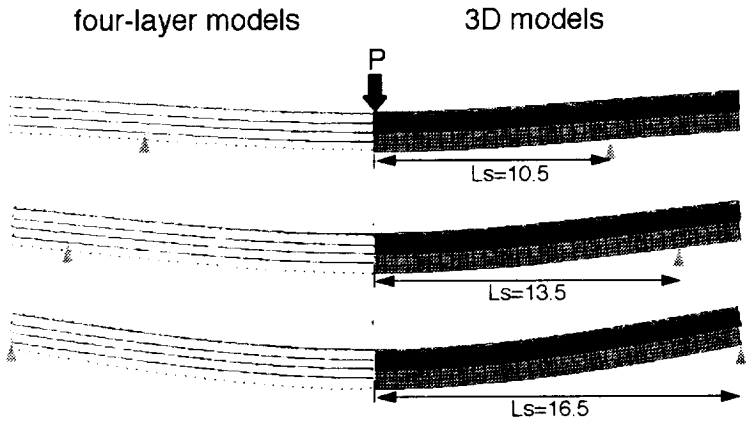

Figure 7. Simulated beam in bending. Results from four-layer models indicate excellent agreement with three-dimensional models at a small fraction of the computational cost.

A composite armored vehicle is designed with a number of structural features that may restrain the transverse shearing at the free edges. Unlike a simple three-point-bending test, few edges of the vehicle are unrestrained. The components are typically bonded and bolted together, and they possess built-in corners. Even the large circular turret opening on the roof is reinforced with a steel and aluminum turret bearing. In a conventional finite element analysis, there is no mechanism for applying end "cap" restraints that prevent shear deformations at the ends. In element-layered and *3D* models, there is enough through-the-thickness freedom to apply end-cap restraints. The two *3D* solutions shown in Fig. 8 illustrate the difference in response between a plate with end-cap restraints in three-point bending and one without these restraints. The plate with end-cap restraints is 85% stiffer than the plate without end-cap restraints.

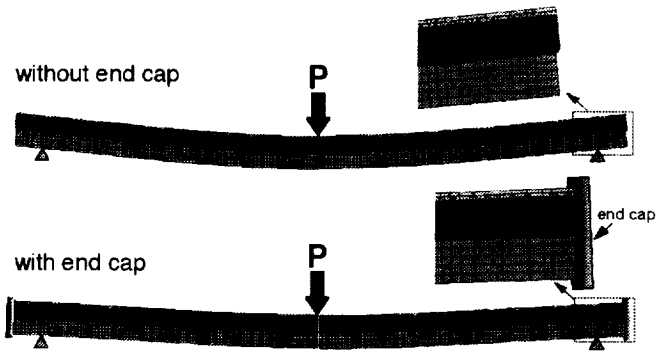

Figure 8. Comparison of plates with and without end-cap restraints in three-point bending. The plate with end caps is 85% stiffer than the plate without end caps.

The graph shown in Fig. 9 summarizes the results of three modeling techniques applied to the plate in three-point bending with varying support spans. Models *L1* consist of conventional, single-layer shell models with a SCF of 0.1 or 0.3. An end-cap restraint cannot be applied to the *L1* models. The *L4* models consist of four-layer shell models with and without end-cap restraints. The *3D* models refer to three-dimensional models with and without end-cap restraints. The results show the normalized stiffness of the plate as a function of support span length. The normalization is with respect to the deflection from beam theory, $EI^{*}PL^{3}$, where EI^{*} is the "equivalent" flexural rigidity of this laminate. The agreement between the *L4* and *3D* models is excellent, as can be observed from the overlap in the results. The shaded area between the results for the models with and without end-cap restraints indicates the uncertainty range of the degree of restraint that may be present at any reinforced edge of the vehicle.

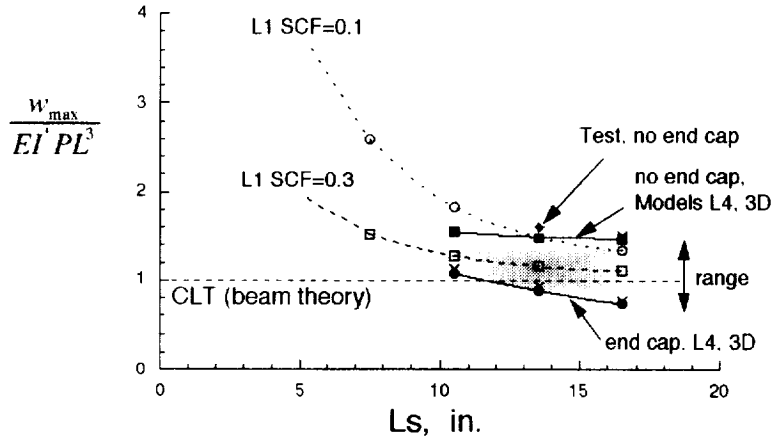

Figure 9. Normalized plate stiffness as a function of support span length. L1 represents sungle-layer models and L4 represents four-layer models.

The element-layering method was automated to transform conventional shell models into multi-layered models. A FORTRAN program was developed to read in information defining the nodes, element connectivities and section properties of a shell model, and to write the new node locations, elements, section properties and MPCs. Decisions such as the number of layers or thicknesses of each layer are made based on the section properties of the original elements. An example of a multi-layered half-model of the test specimen of the rear section of the CAV is shown in Fig. 10. The results of the analysis conducted with this model and the correlation with experiment is presented elsewhere.[5]

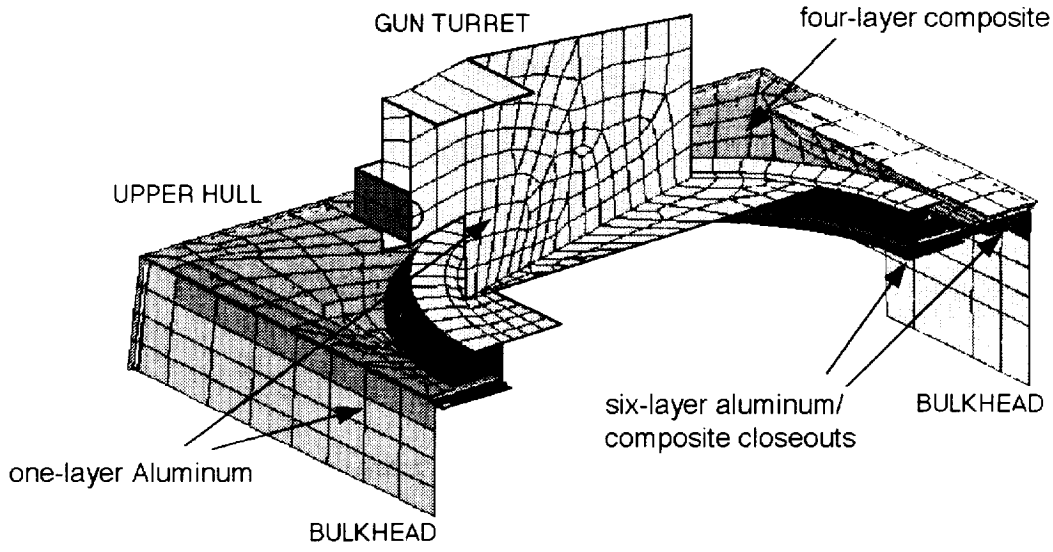

Figure 10. Multi-layered half-model of the rear section of the CAV. Metallic components are modeled with one element layer. Composite sections are modeled with four or six element layers.

Tile Periodicity and Homogenization of the Tile Layer

In addition to the through-the-thickness changes in material properties, the CAV upper hull also exhibits an inplane periodic variation caused by the gaps between the tiles. This periodicity is most apparent in the strains on the surfaces of the laminate. The axial strains shown in Fig. 11 correspond to the outer and inner surfaces of the beam shown in Fig. 2 subjected to three-point bending. The beam in Fig. 2 is a representative section from the CAV upper hull shown in Fig. 1. The surface strains are the strains that can be measured with strain gages bonded to the surfaces of the specimen. The axial strain contours on a portion of the outer surface of the beam, plane ABCD, are shown on the top portion of Fig. 11. The strains on the outer surface along edges CD and AB are plotted with open and closed circles, respectively. These outer surface strains are highly periodic, with strain peaks at the location of the tile gaps. The strains on the inner surface are smooth because the 0.85-inch-thick glass-epoxy inner hull evens out the variations.

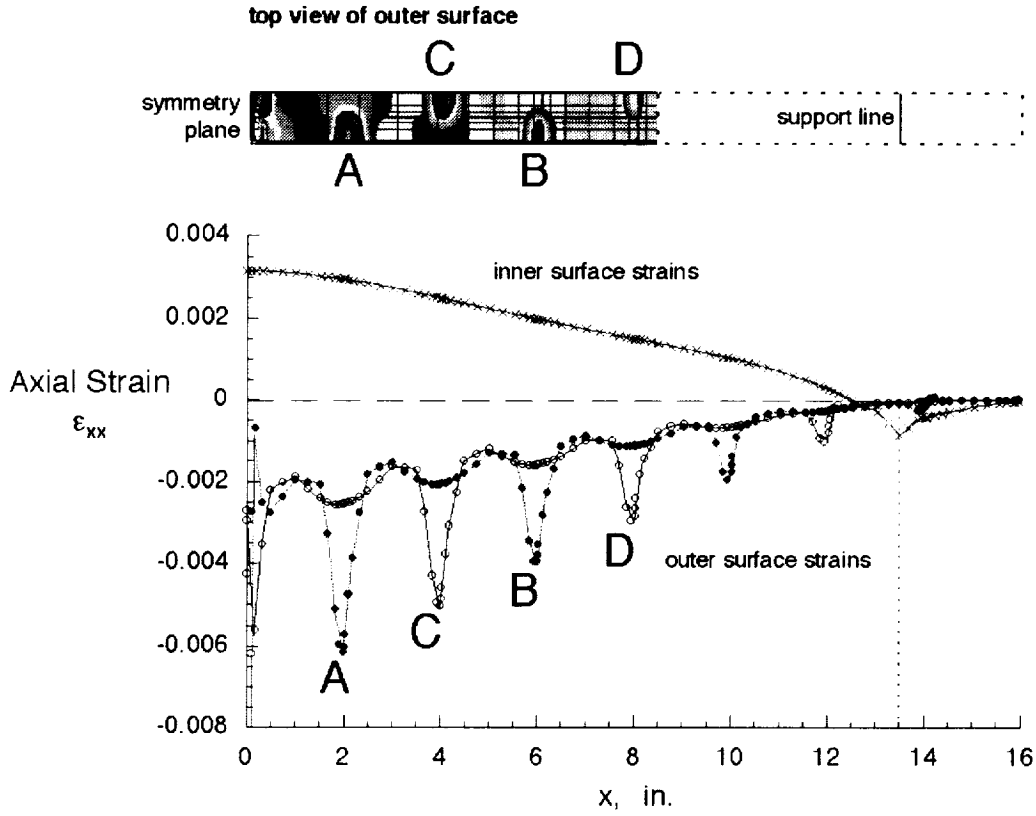

Figure 11. Strains on the surfaces of a beam subjected to three-point bending. The strains on the outer surface have peaks at the gaps between tiles; those on the inner surface are smooth.

While it is essential to account for the deformation of the adhesive gaps, it is not normally possible in a full-vehicle analysis to model each discrete tile and its surrounding adhesive interfaces. Therefore, a homogenized set of material properties was developed that accounts for the complex interactions between the tiles, adhesive and other surrounding materials.

Both square and hexagonal tiles have been considered for the CAV. Square tiles are placed in longitudinally staggered rows, causing a difference in stiffness between the longitudinal and transverse directions. Hexagonal tiles are placed in a honeycomb pattern with a mild orthogonal preference. Homogenized orthogonal properties of the tile-gap layer were obtained numerically by matching the global stiffness of a non-homogenized model (one with tiles and gaps modeled individually) with the stiffness of a homogenized model of the same laminate. The resulting variations of Young's modulus with gap thickness are shown in Fig. 12. It can be observed that the modulus of the homogenized tile layer in the longitudinal direction is twice that in the transverse direction due to "interlocking" of the tiles. The hexagonal tile pattern, which has a milder orthogonal preference, benefits from interlocking in both directions.

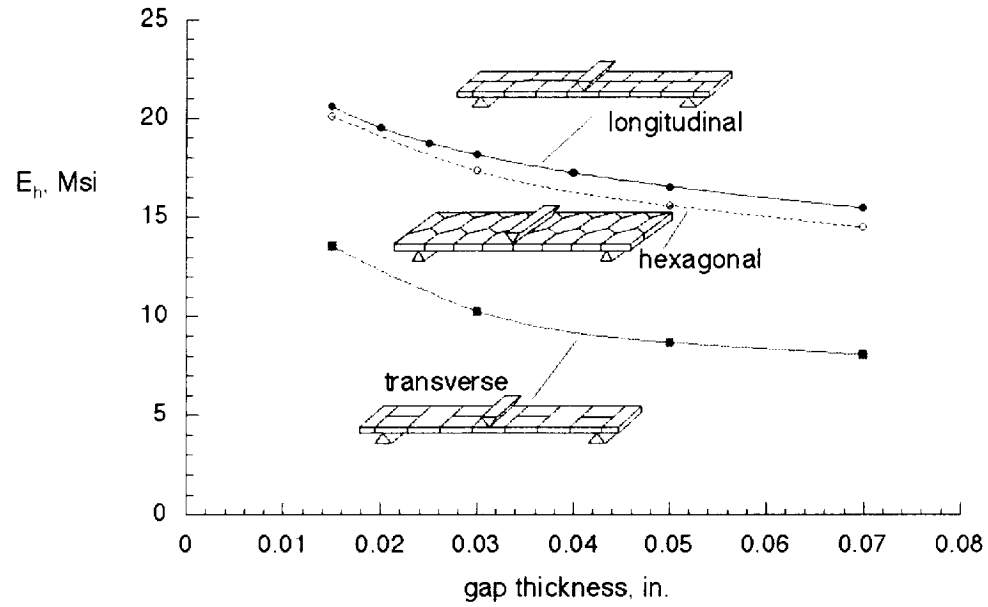

Figure 12. Tile placement pattern and tile shape determine the Young's modulus of the homogenized tile-gap layer. The moduli for three tile configurations are shown as functions of the gap thickness.

Concluding Remarks

The Composite Armored Vehicle (CAV) upper hull achieves its ballistic damage resistance from the interaction of materials with very different stiffnesses. The CAV upper hull consists of layers of glass-epoxy materials, rubber mats, and ceramic tiles. The softness of the rubber mat causes a concentration of transverse shear in that layer, which invalidates the assumptions used for conventional shell finite elements. An analysis was developed based on a method of "element-layering" to predict the response of this layered structure. One of the most important advantages of element-layering over advanced higher-order elements is that it is based on conventional finite elements. Element-layered models are portable from one analysis code to another, which is a prerequisite in a program that involves the computational facilities of several manufacturers and government laboratories. In addition, the method was implemented into an auto-layering program that automatically transforms a conventional shell model into a multi-layered model. A difficulty caused by the discrete tiles is that the adhesive gaps between tiles are too small to be modeled in practical global models. A homogenized model of the tile layers was developed to include the effects of the gaps. The Young's modulus of the homogenized tile layer was computed in both principal directions for square and hexagonal tiles. Used together, the techniques of element-layering and tile-layer homogenization provide a computationally efficient strategy for the finite element analyses of large tile-reinforced CAV components.

References

1. Whitney, J. M., "Shear Correction Factors for Orthotropic Laminates Under Static Load," *Journal of Applied Mechanics, ASME*, Vol. 40, March 1973, pp. 302-304.
2. Averill, R. C., "An Efficient Thick Beam Theory and Finite Element Model with Zig-Zag Sublaminate Approximations," accepted for publication in *AIAA Journal,* 1996.
3. Wang, J. T., Raju, I. S., Dávila, C. G. and. Sleight, D. W, "Computation of Strain Energy Release Rates for Skin-Stiffener Debonds Modeled with Plate Elements," Proceedings of the *AIAA/ASME/ASCE/AHS 34th Structures, Structural Dynamics, and Materials Conference*, April 1993. AIAA Paper 93-1501.
4. Wang, J. T., Raju, I. S., and Sleight, D. W., "Fracture Mechanics Analyses of Composite Skin-Stiffener Debond Configurations with Shell Elements," Proceedings of the *AIAA/ASME/ASCE/AHS/ASC 35th Structures, Structural Dynamics, and Materials Conference,* April 1994. AIAA Paper 94-1389.
5. Pike, T., Lumban-Tobing, F., Smith, C., and Garcia, R., "Composite Armored Vehicle Component Analysis and Test Result Correlation," Proceedings of the *11th DoD/NASA/FAA Conference on Fibrous Composites in Structural Design,* Fort Worth, TX, August 26-29, 1996.

REPORT DOCUMENTATION PAGE

Form Approved
OMB No. 0704-0188

1. AGENCY USE ONLY (*Leave blank*)	2. REPORT DATE	3. REPORT TYPE AND DATES COVERED
	September 1996	Technical Memorandum

4. TITLE AND SUBTITLE
Analysis of Thick Sandwich Shells with Embedded Ceramic Tiles

5. FUNDING NUMBERS
WU 505-63-50-08

6. AUTHOR(S)
Carlos G. Davila; C. Smith; and F. Lumban-Tobing

7. PERFORMING ORGANIZATION NAME(S) AND ADDRESS(ES)
NASA Langley Research Center
Hampton, VA 23681-0001 and
Vehicle Structures Directorate
U.S. Army Research Laboratory
NASA Langley Research Center, Hampton, VA 23681-0001

8. PERFORMING ORGANIZATION REPORT NUMBER

9. SPONSORING / MONITORING AGENCY NAME(S) AND ADDRESS(ES)
National Aeronautics and Space Administration
Washington, DC 20546-0001 and
U.S. Army Research Laboratory
Adelphi, MD 20783-1145

10. SPONSORING / MONITORING AGENCY REPORT NUMBER
NASA TM 110278
ARL-TR-1213

11. SUPPLEMENTARY NOTES
Davila: Langley Research Center, Hampton,VA; Smith and Lumban-Tobing: United Defense, San Jose, CA. Presented at the 11th DoD/NASA/FAA Conference on Fibrous Composites in Structural Design, August 26-30, 1996, Ft. Worth, Texas.

12a. DISTRIBUTION / AVAILABILITY STATEMENT
Unclassified-UnLimited
Subject Category 39

12b. DISTRIBUTION CODE

13. ABSTRACT (*Maximum 200 words*)

The Composite Armored Vehicle (CAV) is an advanced technology demonstrator of an all-composite ground combat vehicle. The CAV upper hull is made of a tough light-weight S2-glass/epoxy laminate with embedded ceramic tiles that serve as armor. The tiles are bonded to a rubber mat with a carefully selected, highly viscoelastic adhesive. The integration of armor and structure offers an efficient combination of ballistic protection and structural performance. The analysis of this anisotropic construction, with its inherent discontinuous and periodic nature, however, poses several challenges. The present paper describes a shell-based "element-layering" technique that properly accounts for these effects and for the concentrated transverse shear flexibilityin the rubber mat. One of the most important advantages of the element-layering technique over advanced higher-order elements is that it is based on conventional elements. This advantage allows the models to be portable to other structural analysis codes, a prerequisite in a program that involves the computational facilities of several manufacturers and government laboratories. The element-layering technique was implemented into an auto-layering program that automatically transforms a conventional shell model into a multi-layered model. The effects of tile layer homogenization, tile placement patterns, and tile gap size on the analysis results are described.

14. SUBJECT TERMS
thick composites shear correction factor
composite armor
element-layering

15. NUMBER OF PAGES
13

16. PRICE CODE
A03

17. SECURITY CLASSIFICATION OF REPORT	18. SECURITY CLASSIFICATION OF THIS PAGE	19. SECURITY CLASSIFICATION OF ABSTRACT	20. LIMITATION OF ABSTRACT
Unclassified	Unclassified		